

Annals of Orthodontics and Periodontics Specialty Volume 4, Page No: 119-132

Available Online at: aopsj.com

Original Article

Impact of Defect Morphology on Alveolar Ridge Preservation: An In Vivo Experimental Study

Qin Tang^{1*}, Kan Wu¹, Xiao-Yu Liu¹

1. Department of Stomatology, The First Affiliated Hospital of Dalian Medical University, Dalian 116011, China.

***E-mail** ⊠ tang.qin.007@163.com

Abstract

This study aimed to assess the bone healing capacity of 1-, 2-, and 3-wall defects after alveolar ridge preservation (ARP) and to determine the effectiveness of ARP in managing compromised extraction sites. Eight beagle dogs were used, with three defect types (1-, 2-, and 3-wall) randomly assigned to the maxillary second, third, and fourth premolars. Each defect was created at either the mesial or distal root of a hemi-sectioned tooth, with the opposing root retained to allow histomorphometric comparison. Sites were randomly treated with either spontaneous healing (SH, control) or ARP (intervention). Each defect group was further divided for healing periods of four or twelve weeks. Histomorphometric data were analyzed using the Mann-Whitney U and Kruskal-Wallis tests, with significance set at P<0.05. Qualitative evaluation indicated greater new bone formation in the apical region than in the coronal region across all defect types and healing intervals. Quantitatively, 3-wall defects in the ARP group showed significantly higher mineralization after 12 weeks (ARP: $61.73\% \pm 7.52\%$; SH: $48.84\% \pm 3.06\%$; P=0.029). Although a trend of increased mineralization was noted with more residual bony walls, this did not reach statistical significance. Within the study's constraints, ARP promoted a higher degree of mineralization in compromised extraction sites compared to spontaneous healing. While the influence of remaining bony walls was modest, their presence appeared to enhance mineralization outcomes in ARP-treated defects.

Key words: Tooth extraction, Bone regeneration, Alveolar ridge augmentation, Histology, Bone substitutes

How to cite this article: Tang Q, Wu K, Liu XY. Impact of Defect Morphology on Alveolar Ridge Preservation: An In Vivo Experimental Study. Ann Orthod Periodontics Spec. 2024;4:119-32. https://doi.org/10.51847/1XJn4GHFHe

Introduction

Following tooth extraction, significant resorption of the alveolar socket has been reported, with reductions averaging 3.79 mm horizontally and 1.24 mm vertically within six months, representing a 29%–63% loss in ridge dimensions [1]. Such shrinkage can complicate dental implant placement and challenge the attainment of primary stability. To address this issue, alveolar ridge preservation (ARP) using bone grafts has been proposed [2,3]. While ARP cannot completely prevent ridge reduction, it aims to maintain adequate bone volume for subsequent implant therapy [4–6].

Extractions are often necessitated by periodontal disease or combined endodontic-periodontal lesions. Teeth affected by periodontitis may result in accelerated ridge resorption and unpredictable healing of the extraction socket [7–9]. Consequently, ARP has been investigated as a strategy to improve the predictability of implant placement in these compromised sites [10–12].



Tang et al.,

Clinical studies have reported a favorable safety profile for ARP in periodontally compromised sockets, with 99.3% of sites either healing uneventfully or managing minor post-treatment infections [13–15]. ARP has been associated with increased bone volume and improved feasibility of implant placement compared with untreated extraction sites. However, histological and radiographic results are variable, likely reflecting differences in healing potential influenced by the number and integrity of remaining bone walls [9,16,17].

Even with ARP, certain compromised sockets may fail to achieve sufficient new bone formation, requiring additional bone augmentation at the time of implant placement [15]. Therefore, understanding how bone wall configuration affects ARP outcomes is crucial for clinicians to optimize treatment planning, inform patients, and enhance collaboration during regenerative procedures.

Prior studies in regenerative dentistry have highlighted a positive correlation between the number of residual bone walls and healing capacity [18–21]. Nevertheless, quantitative data on the relationship between bone wall configuration and ARP outcomes remain limited. Animal studies indicate that in 3-wall defects, new bone can infiltrate graft materials from adjacent native bone within 4 weeks, and resorbable collagen membranes are typically absorbed by 12 weeks [22, 23].

The present study aimed to investigate how 1-, 2-, and 3-wall defects differ in bone healing potential following ARP, assessed at 4 and 12 weeks through histologic analysis.

Materials and Methods

Ethics

All experimental procedures adhered to the principles of the 3 Rs (Replacement, Reduction, and Refinement) and were approved by the Institutional Animal Care and Use Committee of Seoul National University (No. SNU-200619-1-1). Reporting followed the ARRIVE 2.0 guidelines [24].

Sample size determination

Because prior studies comparing ARP outcomes across 1-, 2-, and 3-wall defects are lacking, sample size estimation was based on the assumption that bone formation increases with the number of residual walls. Using G*Power 3.1.9.7 (University of Düsseldorf, Germany), a mean difference of 9% and standard deviation of 3% were applied. With $\alpha = 0.05$ and 80% power, four specimens per group were required. Considering two evaluation periods (four and twelve weeks), eight samples were needed per defect type. Since a single animal could provide all three defect types in the maxillary premolars, eight beagle dogs were sufficient for the study.

Experimental animals

This preclinical study employed eight male beagle dogs, approximately one year old and weighing 10-12 kg. All animals were confirmed to be systemically healthy, with normal periodontal status and dentition, prior to inclusion. Before the procedures, the dogs underwent a 2-week acclimatization period at the research facility. Each animal was housed individually in indoor kennels measuring $90 \times 80 \times 80$ cm, provided with unlimited access to water, and fed a standard pellet diet.

Study design

The study evaluated three defect configurations—1-wall, 2-wall, and 3-wall—randomly assigned to the maxillary second, third, and fourth premolars (Figure 1A). A split-mouth design was implemented, with spontaneous healing (SH) serving as the control and alveolar ridge preservation (ARP) as the experimental treatment. For each dog, one defect was created at the mesial root on the left side, and the other at the distal root on the right side, allowing the preserved contralateral root to serve as a reference for histomorphometric comparison. Full blinding was not possible during or after the procedures due to the visible presence of the bone graft material.

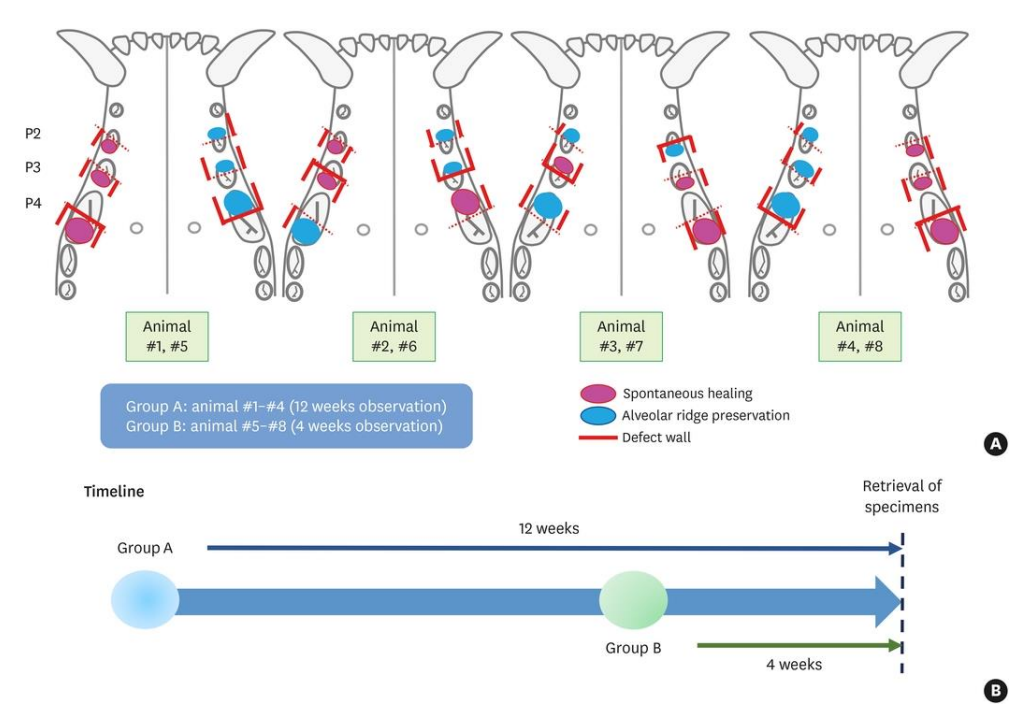


Figure 1. In this split-mouth experiment, one hemi-sectioned root in each dog was randomly designated for either the spontaneous healing (SH) control or the alveolar ridge preservation (ARP) intervention, with the opposite root retained to serve as an internal reference for alveolar ridge evaluation

Experimental materials

For the ARP sites, ridge preservation was performed using collagenated deproteinized porcine bone mineral (THE Graft Collagen, Purgo, Seongnam, Korea). A crosslinked collagen membrane (The Cover, Purgo) was carefully trimmed to fit the defect dimensions and placed over the area, followed by placement of the bone graft material to fill the socket.

Study procedures

The overall experimental timeline is depicted in **Figure 1B**. In each group, four dogs underwent root hemisection and creation of standardized alveolar defects. Each defect was randomly assigned to either SH or ARP, with designated healing intervals of 4 or 12 weeks.

Anesthesia protocol

Prior to surgery, general anesthesia was induced using an intravenous combination of tiletamine hydrochloride and zolazepam hydrochloride (0.1 mg/kg, Zoletil, Virbac, France), xylazine (2.3 mg/kg, Rompun, Bayer Korea), and atropine sulfate (0.05 mg/kg, Jeil Pharm., Korea). Local anesthesia was then administered via infiltration with 2% lidocaine containing 1:1,000,000 epinephrine (Huons, Seongnam, Korea).

Defect creation and ridge preservation procedure

Surgical interventions began with intracrevicular incisions in the maxillary premolar area and careful reflection of full-thickness flaps (Figure 2). The second, third, and fourth maxillary premolars (PM2–PM4) were hemisected using a diamond bur (TC-21, Kiyohara Industrial Park, Japan). Root canal therapy was performed on the portion of the root intended for retention using 25 mm K-files (#15 and #20, MANI, Japan) and Ni-Ti Protaper files (SX, F1–F3, Dentsply Maillefer, Switzerland). After thorough canal preparation, a calcium hydroxide–based sealer (cleaniCal, Maruchi, Korea) was applied, and the root canal was temporarily sealed with a cotton pellet and intermediate restorative material (Dentsply Sirona, USA).

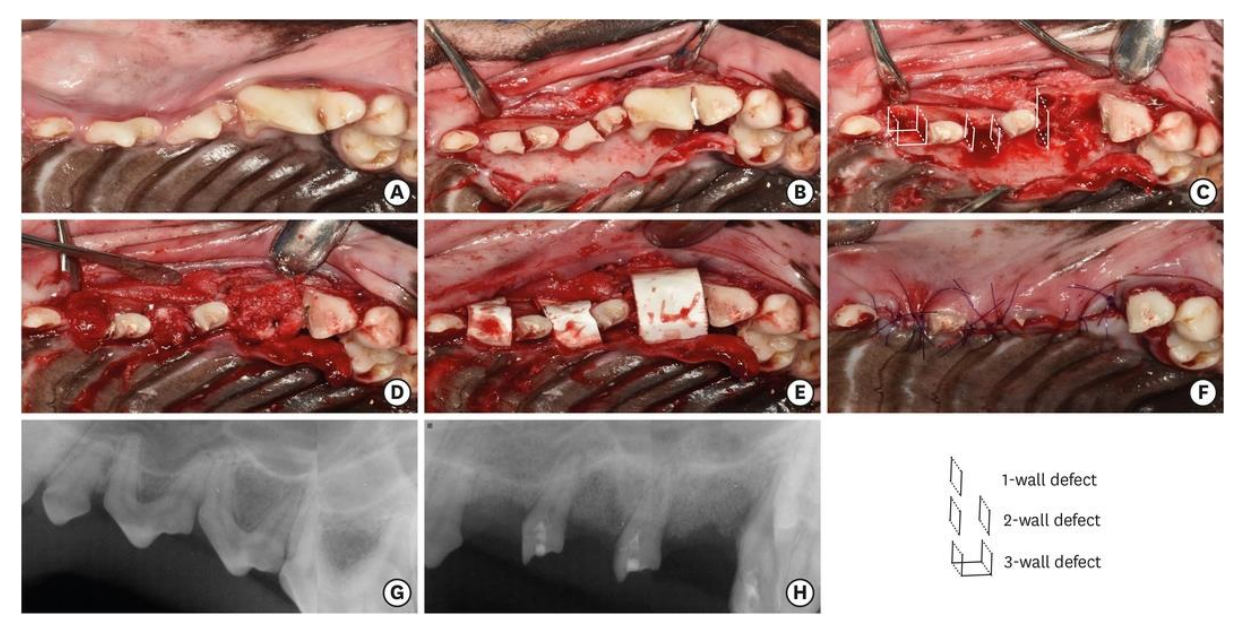


Figure 2. The workflow of the study is illustrated through clinical and radiographic images: preoperative views (A), intraoperative steps showing defect creation after hemi-sectioned root removal (B, C), application or omission of alveolar ridge preservation in a randomized split-mouth setup (D–F), and periapical radiographs taken before and after surgery (G, H)

Defect preparation

At each designated experimental site, the targeted root was extracted, and defects were prepared according to the assigned configuration using a #4 round bur. The three defect types were defined as:

- 1-wall defect: buccal, lingual, and mesial (or distal) walls removed, leaving the root fully exposed.
- 2-wall defect: only the buccal and lingual walls removed.
- 3-wall defect: only the buccal wall was removed, preserving the remaining bone walls.

Measurements of defect height (10 mm) and the mesiodistal width of the root were recorded using a Williams probe. The exposed root surfaces were meticulously planed to remove all remnants of the periodontal ligament. Sites allocated to ARP received collagenated deproteinized porcine bone mineral, covered with a double-layered crosslinked collagen membrane, and the flap was advanced for tension-free primary closure, secured with 4/0 Vicryl sutures (Ethicon Inc., Raritan, NJ, USA).

Postoperative management

Following surgery, animals were treated with intravenous antibiotics (Cefazolin, 20 mg/kg) and analgesics (Toranzin, 5 mg/kg) along with antispasmodics (atropine sulfate, 0.05 mg/kg). For three days postoperatively, oral antibiotics (Amoxicillin, 500 mg) and analgesics (Ibuprofen, 400 mg) were administered in the diet. Sutures were removed after 10 days, and oral hygiene was maintained using 0.12% chlorhexidine gluconate applied twice weekly.

Euthanasia and sample collection

Animals were sacrificed at either 4 or 12 weeks after surgery via carotid injection of potassium chloride (75 mg/kg). Block biopsies including the surgical site and the retained root were harvested for histological processing.

Histological processing

Samples were fixed in 10% neutral buffered formalin for two weeks, washed with sterile water, and decalcified in 5% formic acid for ten days. Following dehydration in graded ethanol, the specimens were embedded in paraffin. Blocks included the

remaining root and surrounding surgical site, and the central buccolingual section was selected for analysis. Sections 5 μ m thick were cut and stained with Masson trichrome to allow both histological observation and quantitative assessment.

Histological and histomorphometric evaluation

Digital images of the slides were captured and analyzed using CaseViewer (3DHISTECH, Budapest, Hungary). Rectangular regions of interest (1 mm × 1 mm) were defined in apical, middle, and coronal portions of the defects. Symmetry with the contralateral root allowed alignment and superimposition for accurate positioning of ROIs relative to the sinus floor and residual alveolar contours. Vertical placement of the ROIs was measured from the midpoint of the buccopalatal alveolar crest to the root apex. Images were magnified ninefold, and the proportion of newly formed bone and remaining graft material within each ROI was calculated using ImageJ software (NIH, Bethesda, MD, USA).

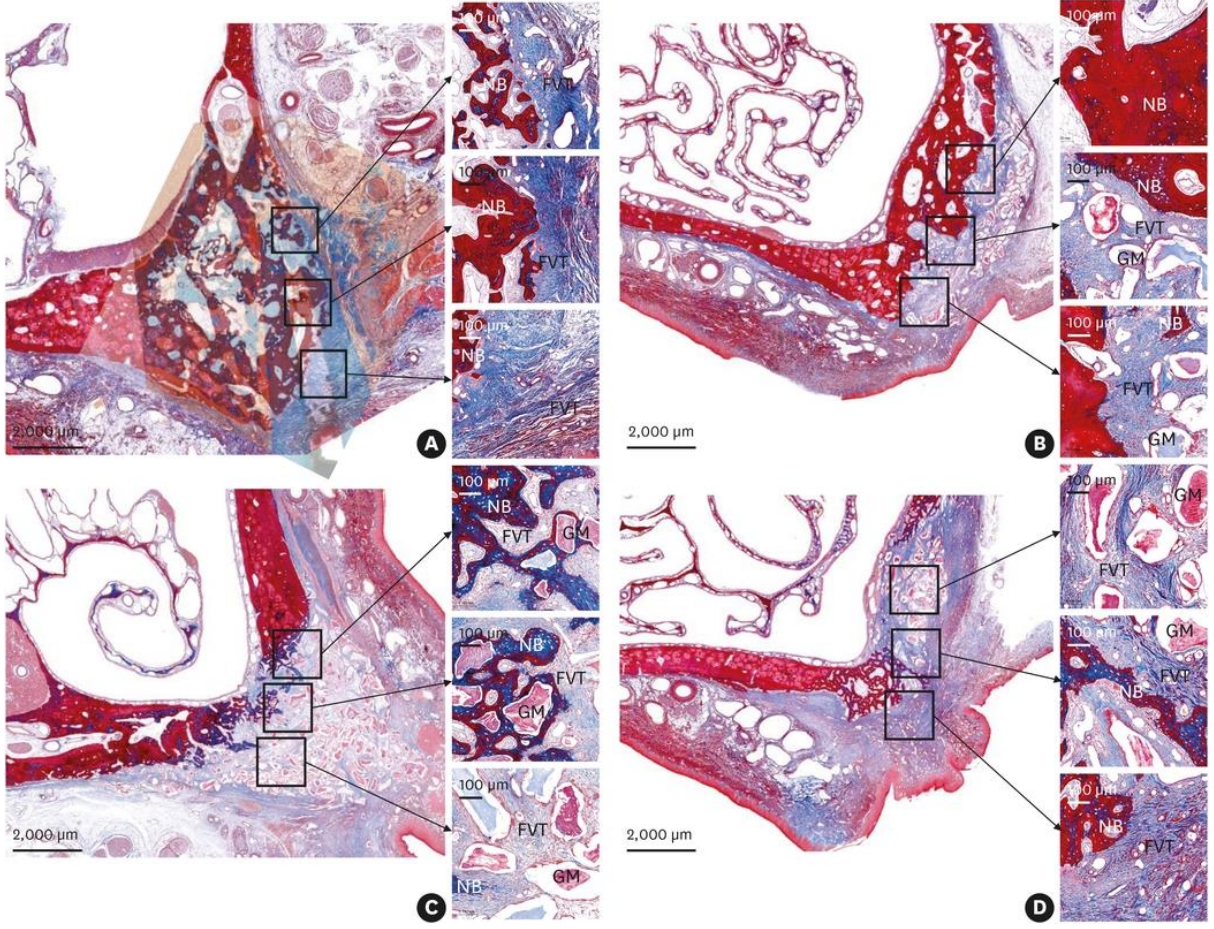


Figure 3. Examples of histological healing at four weeks across different defect types. (A) A 3-wall defect that healed spontaneously, displayed alongside the preserved contralateral root for comparison. (B) A 3-wall defect treated with alveolar ridge preservation, shown in alignment with the contralateral root. (C) A 2-wall defect receiving alveolar ridge preservation, superimposed with the corresponding contralateral root. (D) A 1-wall defect after alveolar ridge preservation, presented alongside the retained contralateral root for reference.

Legend: NB = new bone, FVT = fibrovascular connective tissue, GM = graft material

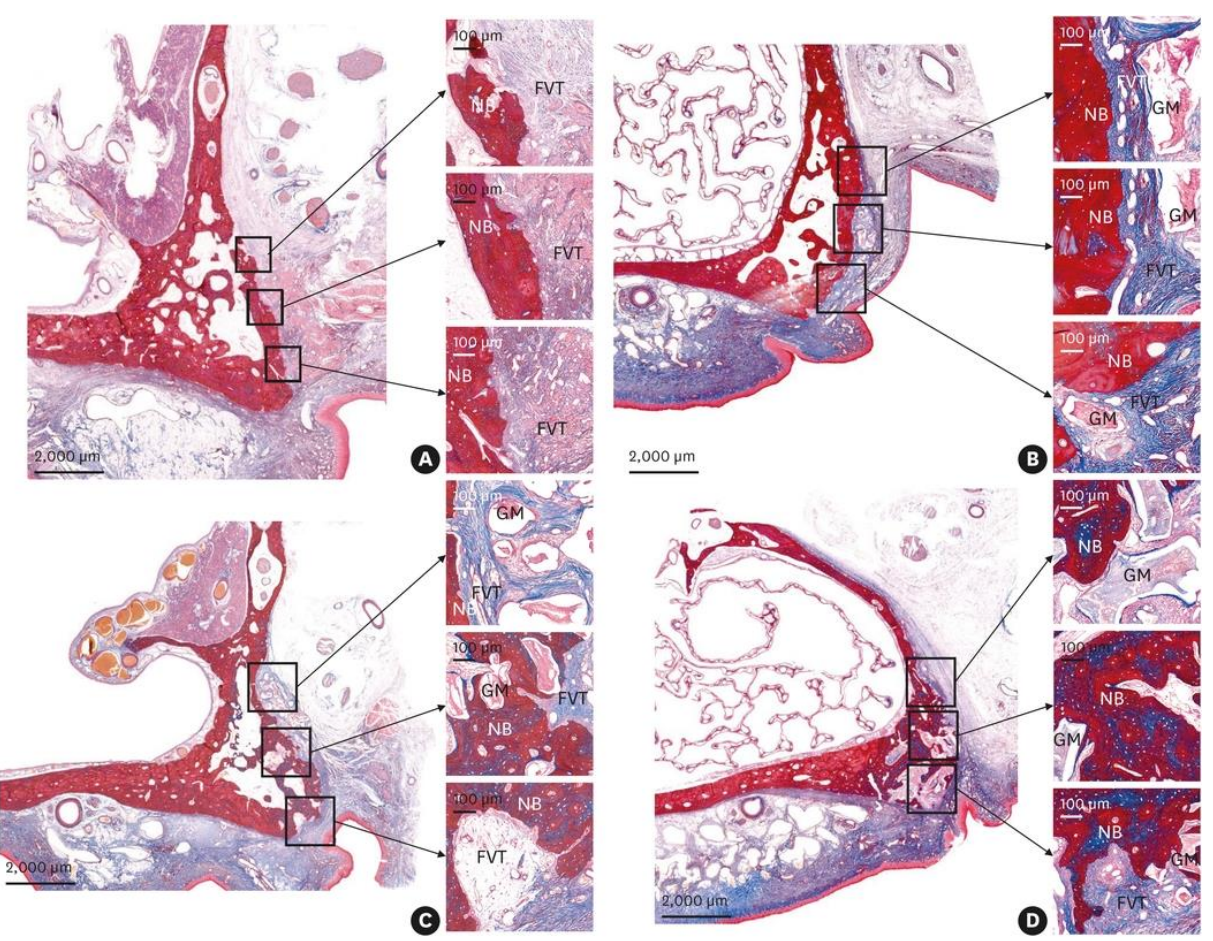


Figure 4. Histological examples of socket healing at twelve weeks for different defect configurations. (A) Spontaneously healed 3-wall defect aligned with the contralateral preserved root for reference. (B) 3-wall defect treated with alveolar ridge preservation, displayed alongside the corresponding contralateral root. (C) 2-wall defect managed with ARP, compared to the contralateral root. (D) 1-wall defect after ARP, shown in relation to the preserved contralateral root.

Abbreviations: NB = new bone, FVT = fibrovascular connective tissue, GM = graft material

Quantitative histometric assessment

For measurement purposes, the contralateral root was vertically overlaid, spanning from the alveolar crest to a point 3 mm below it. Within this framework (**Figure 5**), three areas were defined:

- Reference area: the entire region bounded by the inner surface of the palatal bone and the outer edge of the buccal bone on the superimposed image.
- Augmented area: the portion within the reference area occupied by both graft material and newly formed bone.
- Regenerated area: the segment within the reference area containing only newly formed bone.

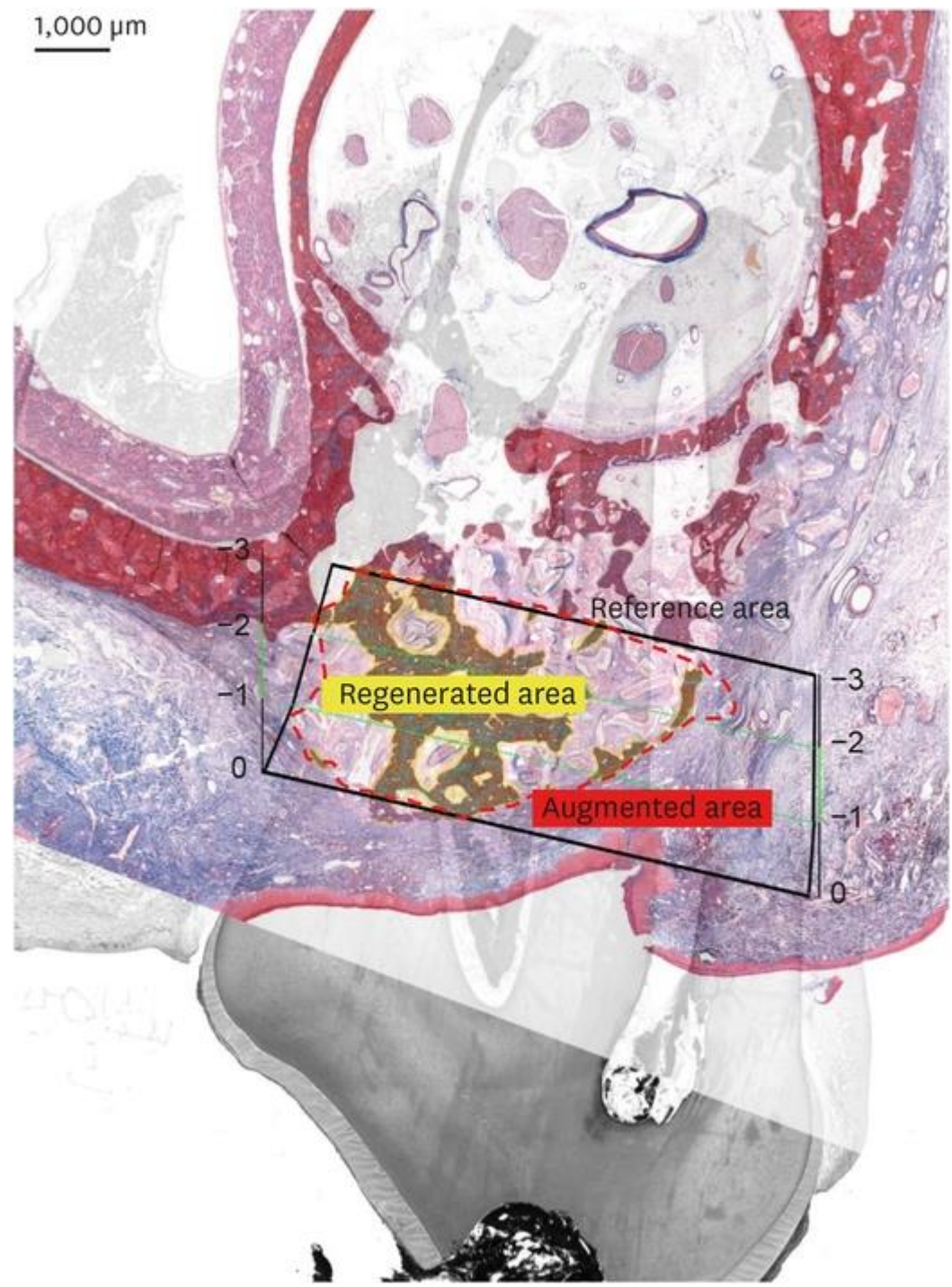


Figure 5. Example of histological analysis used for qualitative evaluation. Images from the corresponding contralateral site of the same tooth were overlaid to establish spatial reference. The reference area was delineated based on the vertical positions of the buccal and palatal bone walls surrounding the opposite root. Within this area, the regenerated bone and augmented regions are highlighted with yellow and red dotted lines, respectively

The sizes of the regenerated and augmented regions within the reference zone were quantified using ImageI, and the mineralization percentage within the augmented area was determined using the following calculation:

$$-\textit{Mineralization Percentage} = \frac{\textit{Regenerated Area}}{\textit{Reference Area}} \times 100 \tag{1}$$

For both qualitative and quantitative histometric evaluations, a specialist performed three separate measurements per site each week, and the mean of these measurements was used for analysis.

Statistical analysis

Data were analyzed using SPSS software (version 25.0, IBM Corp., Armonk, NY, USA). Results are presented either as mean ± standard deviation or as median with interquartile range (minimum-maximum). The Mann-Whitney U test and Kruskal-Wallis test were applied for histomorphometric comparisons. To explore factors potentially influencing the percentage of mineralized tissue, the generalized estimating equation (GEE) approach was used. Statistical significance was defined as P < 0.05.

Results

Clinical observations

All eight beagle dogs completed the 4- and 12-week healing intervals. Healing progressed uneventfully at every experimental site, with no evidence of inflammation. Greater volumetric reduction was noted in 1-wall defects compared with 2- and 3wall defects, irrespective of whether ARP was applied.

Histological findings

All experimental defects were free of inflammatory signs, and areas of augmentation showed integration of graft material with newly formed bone. Bone mineralization increased over time. In ARP-treated sites, trabecular new bone was observed within the augmented regions, with inter-trabecular spaces occupied by residual graft material and connective tissue containing blood vessels. Bone formation was more pronounced at deeper levels, moving away from the alveolar crest.

Histomorphometric evaluation

Qualitative analysis of SH and ARP groups

Table 1 summarizes qualitative histometric comparisons among 1-wall, 2-wall, and 3-wall defects at both SH and ARP sites. At four weeks, there were no significant differences in bone formation among the three defect types for either SH or ARP. Similarly, after 12 weeks, differences between defect types remained non-significant. Across all sites at four weeks, new bone formation was consistently higher in the apical region than in the coronal region.

Table 1. Qualitative histometric analysis of SH and ARP groups									
Time	Location	Defect	SH			ARP			
Time			NB	GM	FVT	NB	GM	FVT	
4 weeks	Apical	1-wall	61.53±8.41	-	38.48 ± 8.41	48.5±33.90	5.35 ± 10.7	46.15±23.98	
			63.15 (51–69), 16		36.35 (31–50), 16	58.60 (0–77), 61	0 (0–21), 16	41.40 (23–79), 45	
		2-wall	24.93±25.09	-	75.08±25.09	63.35±15.11	3.25±6.5	33.40±18.02	
			20.00 (0–60), 46		80 (40–100), 46	66.15 (43–78), 28	0 (0–13), 10	29.50 (17–57), 34	
		3-wall	26.70±23.69		73.30±23.69	45.40±21.84	5.1±6.13	49.50±17.49	
			25.05 (0–57), 45	-	74.95 (43–100), 45	46.20 (20–70), 42	4.05 (0–12), 11	47.65 (30–72), 33	
		P value	0.087	-	0.087	0.551	0.915	0.472	
	Middle	1-wall	40.58±11.03	-	59.43±11.03	25.50±22.92	9.35±9.13	65.15±19.93	

$ \begin{tabular}{ c c c c c c c c c c c c c c c c c c c$
$ \begin{array}{c ccccccccccccccccccccccccccccccccccc$
Coronal Coronal I-wall $0.625 (5-26), 19 = 0.00 = $
Coronal Coronal P value $0.467 - 0.467 - 0.915 - 0.904 - 0.841 - 0.467 - 0.915 - 0.904 - 0.841 - 0.467 - 0.35 - 0$
Coronal 2-wall $27.30 (0-50)$, 44 $- 72.70 (50-100)$, 44 $0 (0-14), 10$ $17.85 (2-33)$, $82.15 (67-84), 13$ 7.95 ± 9.25 92.05 ± 9.25 3.95 ± 4.64 14.25 ± 7.81 81.80 ± 6.71 $17.25 (0-17), 17$ $- 92.75 (83-100)$, $17.85 (2-33)$, 1
Coronal 44 4 44 0 (0-14), 10 23 82.13 (67-84), 13 $\frac{7.95 \pm 9.25}{3.95 \pm 4.64}$ 14.25 ± 7.81 81.80 ± 6.71 81.80 ± 6.71 7.25 (0-17), 17 - 92.75 (83-100), 17 17 17 17 17 17 17 18 18 18.55 (74-90), 13 18 18 18 18 18 18 18 18 18 18 18 18 18
$ \begin{array}{c ccccccccccccccccccccccccccccccccccc$
$ \begin{array}{c ccccccccccccccccccccccccccccccccccc$
$ \begin{array}{c ccccccccccccccccccccccccccccccccccc$
$\begin{array}{c ccccccccccccccccccccccccccccccccccc$
35 35 39 7.50 (0-21), 19 27.8 (7-64), 46 39.13±14.94 60.88±14.94 48.50±24.69 21.0±13.65 30.50±11.72 2-wall 34.25 (27-61), - 65.75 (39-73), 43.70 (27-80), 22.25 (6-34), 33.1 (14.42) 46
Apical 2-wall 34.25 (27–61), - 65.75 (39–73), 43.70 (27–80), 22.25 (6–34), 33.1 (14–42) 46
Anical $(-, -)$ $(-, -)$ $(-, -)$ $(-, -)$ $(-, -)$ $(-, -)$ $(-, -)$ $(-, -)$ $(-, -)$ $(-, -)$ $(-, -)$ $(-, -)$
51.97±24.81 48.03±24.81 75.83±1.80 3.55±4.27 20.63±5.5
3-wall 51.65 (30–75), 44 48.35 (25–70), 75.35 (74–78), 2.80 (0–9), 8 22.35 (13–25), 10
P value 0.551 - 0.551 0.334 0.128 0.551
42.55±19.17 57.45±19.17 29.05±12.62 16.73±11.53 54.23±21.68
1-wall $42.70 \ (21-63)$, $57.30 \ (37-79)$, $24.00 \ (20-48)$, $20.08 \ (0-25)$, $20.08 \ (27-80)$, 20.08
36.22±19.57 63.78±19.57 46.93±17.18 25.20±9.74 27.88±12.52
12 weeks Middle 2-wall 34.85 (14–62), - 65.15 (39–86), 47.15 (31–63), 28.01 (11–34), 31.00 (11–39), 28
39.63±16.84 39.38±26.92 51.58±33.06 27.73±26.17 20.7±7.58
3-wall 43.30 (16–56), 49.95 (0–58), 46 52.00 (12–90), 24.95 (0–61), 23.05 (10–27), 14
P value 0.874 - 0.368 0.309 0.537 0.037 ^{b)}
49.75±6.29 50.25±6.29 12.38±8.40 9.78±19.55 77.85±18.20
1-wall 47.50 (45–59), 11 52.50 (41–55), 9.00 (7–25), 14 0 (0–39), 29 82.45 (53–93), 34
37.53±29.30 54.18±42.22 37.98±22.54 26.65±20.44 35.38±5.64
Coronal 2-wall 39.90 (4-67), 56 - 60.10 (0-97), 81 44.25 (6-58), 24.00 (5-54), 36.95 (27-40), 10
39.75±35.01 35.25±32.79 25.48±20.40 31.25±20.39 43.27±28.00
3-wall 36.85 (0–85), 65 - 38.10 (0–65), 60 27.10 (0–48), 30.10 (9–56), 42.30 (10–79), 52
P value 0.668 - 0.828 0.390 0.227 0.037 ^{a)}

Data are expressed as mean ± standard deviation or as median (minimum-maximum) with interquartile range.

Abbreviations: SH = spontaneous healing, ARP = alveolar ridge preservation, NB = new bone, GM = graft material, FVT = fibrovascular connective tissue. Notes: a) P < 0.05 for comparisons between 1-wall and 2-wall groups; b) P < 0.05 for comparisons between 1-wall and 3-wall groups.

Quantitative histometric analysis of SH and ARP groups

Quantitative evaluation was conducted to compare 1-wall, 2-wall, and 3-wall defects at sites treated with either spontaneous healing (SH) or alveolar ridge preservation (ARP), as summarized in **Table 2**. A total of twelve samples from each healing interval (four weeks and twelve weeks) were included in the analysis. At the 4-week time point, no statistically significant differences in mineralization percentages were observed between SH and ARP sites. Likewise, within each group, defect type (1-wall, 2-wall, or 3-wall) did not show significant differences in the percentage of mineralized tissue at 4 weeks.

Table 2. Quantitative histometric analysis of SH and ARP groups

Time	Variables	Defect	SH	ARP	P value	
		1-wall -	11.73±4.12	10.30 ± 2.98	1	
		1-waii	11.45 (7.87–16.15), 7.64	9.16 (8.16–14.7), 5.07		
		2-wall -	9.42 ± 2.29	12.36 ± 8.76	- 0.886	
	Reference area (mm ²)	Z-waii	8.95 (7.19–12.58), 4.26	8.46 (7.1–25.4), 14.12		
		3-wall -	12.13±8.07	13.86 ± 9.05	- 1	
		J-waii	8.42 (7.45–24.22), 12.77	10.22 (7.85–27.16), 15.37		
_		P value	0.779	0.694		
		1-wall		7.41±1.10		
		1-waii		7.34 (6.13–8.83), 2.05		
		2-wall		7.15±3.34		
	Augmented area (mm ²)		-	6.19 (4.41–11.82), 6.11		
		3-wall	-	11.62±9.75		
				7.81 (4.99–25.88), 16.75		
_		P value	-	0.794		
		1-wall -	3.94 ± 1.43	4.18±1.56	- 1	
		1-waii	4.39 (1.89–5.09), 2.55	3.97 (2.54–6.25), 2.97		
		2-wall	5.04 ± 2.90	4.08 ± 4.58	- 0.886	
4 weeks	Regenerated area (mm ²)	z-wan	4.16 (2.6–9.26), 5.03	3.1 (0–10.14), 8.59		
		3-wall -	3.97 ± 2.22	4.84±4.62	 - 1	
		3-waii	3.95 (1.28–6.69), 4.19	2.99 (1.73–11.66), 7.78	1	
_		P value	0.874	0.841		
	Augmented/reference area (%)	1-wall		76.00±22.67		
			-	76.84 (50–100), 43		
		2-wall	-	63.43±13.55		
				63.92 (46–79), 26		
		211		77.22±14.72		
		3-wall	-	75.02 (64–95), 28		
_		P value	-	0.39		
		1-wall -	35.27±14.39	42.50±19.33	- 0.486	
			30.5 (24.0–55.0), 26	34.5 (30–71), 32		
	Mineralization percentage (%)	2-wall -	52.25±19.00	47.25±27.14	- 0.343	
			53.5 (28.0–74.0), 36	53 (12–71), 51		
		3-wall -	35.50±16.36	32.5±13.77	- 0.686	
			38.0 (16.0–50.0), 31	36.5 (14–43), 51		
		P value	0.234	0.788		
	Reference area (mm²)	1-wall	12.01±2.93	16.01±8.13	0.686	
		1-wall	12.73 (7.93–14.67), 5.41	15.98 (8.82–23.28), 14.28	0.080	
		2-wall -	9.35±2.04	11.53±6.02	- 1 - 1	
12 weeks			8.91 (7.55–12.02), 3.83	8.91 (7.77–20.53), 9.65		
		3-wall —	12.28±7.72	10.04±2.54		
			10.14 (5.77–23.11), 14.15	9.17 (8.12–13.74), 4.47		
		P value	0.437	0.309		
		1-wall		10.49±2.62		
				10.62 (7.2–13.55), 5.01		
	Augmented area (mm ²)	2-wall		7.65±2.69		
	Augmented area (IIIIII)	∠-wan	-	6.51 (5.93–11.67), 4.43		
		3-wall		8.15±1.36		
			-	7.78 (7.01–10.05), 2.5		

	P value	N/A	0.174		
Regenerated area (mm ²)	1-wall	3.65±0.63	6.81±3.32	- 0.200	
		3.72 (2.82–4.34), 1.18	7.04 (3.2–9.98), 6.2		
	2-wall —	3.94±0.82	5.35±1.19	- 0.114	
		3.77 (3.22–5.01), 1.55	5.14 (4.12–6.99), 2.18		
	3-wall —	5.83±3.38	6.09±0.96	- 0.486	
		4.85 (3.01–10.63), 6.16	6.14 (4.87–7.23), 1.78		
	P value	0.551	0.779		
	111		72.18±23.27		
	1-wall	-	70.48 (48–100), 45		
Augmented/reference area (%)	2-wall		69.91±10.16		
			71.17 (57–80), 19		
	3-wall		82.48 ± 12.12	_	
		-	78.39 (73–100), 21	_ <u>-</u>	
	P value	-	0.469		
Mineralization percentage (%)	1-wall —	34.06±15.07	43.15±7.08	- 0.343	
		31.16 (19.0–55.0), 28	41.75 (36.0–53.0), 13		
	2-wall —	42.89±8.98	50.65±11.29	- 0.343	
		41.08 (34.0–55.0), 16	55.24 (34.0–58.0), 19	- 0.343	
	3-wall —	48.84 ± 3.05	61.73±7.5	- 0.029 ^{a)}	
		48.59 (46.0–52.0), 6	61.8 (53.0–71.0), 14		
	P value	0.292	0.077		

Data are reported as mean ± standard deviation or median (minimum-maximum) with interquartile range.

Abbreviations: SH = spontaneous healing; ARP = alveolar ridge preservation; N/A = not available.

Mineralization percentage calculated as:

At 12 weeks, no significant differences in mineralization were observed between SH and ARP sites for 1-wall and 2-wall defects. However, in 3-wall defects, the ARP group showed a significantly higher mineralization percentage compared to SH (ARP: $61.73\% \pm 7.52\%$ vs. SH: $48.84\% \pm 3.06\%$, P = 0.029). Within each group, mineralization tended to increase with the number of remaining bone walls, although these differences did not reach statistical significance. Generalized estimating equation (GEE) analysis revealed that both defect configuration and healing duration had a significant effect on mineralization. Furthermore, significant interaction effects were observed among defect type, treatment modality, and healing time, as detailed in **Table 3**.

Table 3. Predictors of mineralization percentage

Variables	Wald	P value
Defect type (1-, 2-, or 3-wall)	14.30	< 0.001
Healing time (4 or 12 wk)	5.40	0.02
Intervention (SH or ARP)	0.12	0.72
Defect type × intervention	9.32	0.01
Defect type × healing time	40.85	< 0.001
Healing time × intervention	5.20	0.02
Defect type × healing time × intervention	57.95	< 0.001

Analysis was conducted using the generalized estimating equation (GEE) method.

Abbreviations: SH = spontaneous healing; ARP = alveolar ridge preservation.

Discussion

This study aimed to investigate the bone healing capacity of 1-, 2-, and 3-wall defects following alveolar ridge preservation (ARP) after tooth extraction using histomorphometric analysis. After 12 weeks, sites treated with ARP showed a larger regenerated area and a higher proportion of mineralized tissue compared with spontaneous healing (SH). Notably, in 3-wall defects, the ARP group exhibited a statistically significant increase in mineralization relative to SH at the same time point. Although not reaching significance, both SH and ARP groups showed a trend toward greater mineralization at 12 weeks as the number of remaining bony walls increased.

a) P < 0.05.

Tang et al.,

Previous research has primarily addressed volumetric changes, demonstrating that ARP can limit both horizontal and vertical alveolar ridge resorption compared with untreated sites [25, 26]. Clinical studies have similarly reported that ARP is effective in preserving ridge dimensions in periodontally compromised extraction sites [15]. However, the specific influence of the number of residual bony walls on ARP outcomes remains underexplored. In the current study, a higher percentage of mineralization was generally observed as the number of bony walls increased in both SH and ARP groups, although this did not achieve statistical significance. Significantly, in 3-wall defects, mineralization was greater in ARP-treated sites than in SH (P = 0.029), suggesting that the remaining bone walls may serve as a key source of regenerative potential during ARP. Healing duration is a known factor in new bone formation. Previous studies have shown that longer healing periods are associated with increased bone regeneration [27, 28]. Consistent with this, our findings demonstrated that the 12-week healing group exhibited a higher percentage of mineralized tissue than the 4-week group, irrespective of defect type. This indicates that optimal osteogenesis, potentially influenced by the amount of residual bone, is more likely to occur after 12 weeks rather than 4 weeks.

Bone regeneration is facilitated by the provisional matrix, vascular networks, and multipotent macrophages derived from adjacent intact bone [29]. Prior studies have shown that a greater number of intact bony walls enhances the healing environment in guided bone regeneration procedures [30]. Accordingly, ARP in 3-wall defects is expected to support higher regeneration rates than in 1-wall defects. In our study, mineralization tended to increase with the number of remaining walls, although the difference was not statistically significant.

Porcine-derived bone grafts, as used in this study, have been reported to provide comparable bone formation and volume stability to bovine bone [31, 32]. However, their resorption patterns may vary, with continuous resorption occurring without clear osteoclastic activity at certain intervals [33, 34], which may have contributed to variability in outcomes. Future studies should further examine the resorption behavior of the porcine graft material employed.

During the ARP procedures, flaps were reflected and sutured to achieve primary closure due to the acute defect model. Primary wound closure may have influenced mineralization by providing soft tissue stability, potentially reducing the effect of defect wall configuration. Although studies on periodontally compromised sockets have shown similar bone formation and ridge preservation with or without primary closure [35], the role of soft tissue stability in ARP outcomes should not be overlooked.

Several limitations should be acknowledged. First, the small sample size in each subgroup (defect type and intervention) may have limited statistical power, possibly explaining why defect type did not reach significance as a predictor of mineralization. Second, contralateral ridge morphology in the dogs may have differed from the original site, making precise 3D alignment of histological sections challenging. Third, anatomical factors such as irregular palatal bone or sinus shape may affect ARP outcomes; the lack of a palatal vault in dogs complicates complete palatal wall removal. Using mandibular teeth could help reduce variability in future studies. Fourth, three-dimensional evaluation via micro-computed tomography (micro-CT) was not performed, which could enhance quantitative analysis of bone regeneration.

Within these limitations, ARP appears to enhance mineralization compared with SH in compromised extraction sites. Factors including defect configuration, healing time, and the application of ARP seem to influence bone regeneration. While the presence of residual bony walls had a limited effect, their existence appeared to modestly support increased mineralization during ARP treatment.

Acknowledgments: None

Conflict of interest: None

Financial support: None

Ethics statement: None

References

- 1. Tan WL, Wong TLT, Wong MCM, Lang NP. A systematic review of post-extractional alveolar hard and soft tissue dimensional changes in humans. Clin Oral Implants Res. 2012;23(Suppl 5):1–21.
- 2. Aimetti M, Romano F, Griga FB, Godio L. Clinical and histologic healing of human extraction sockets filled with calcium sulfate. Int J Oral Maxillofac Implants. 2009;24(5):902–9.
- 3. Barone A, Aldini NN, Fini M, Giardino R, Calvo Guirado JL, Covani U. Xenograft versus extraction alone for ridge preservation after tooth removal: a clinical and histomorphometric study. J Periodontol. 2008;79(8):1370–7.
- 4. Darby I, Chen ST, Buser D. Ridge preservation techniques for implant therapy. Int J Oral Maxillofac Implants. 2009;24(Suppl):260–71.
- Bienz SP, Ruales-Carrera E, Lee WZ, Hämmerle CHF, Jung RE, Thoma DS. Early implant placement in sites with ridge preservation or spontaneous healing: histologic, profilometric, and CBCT analyses of an exploratory RCT. J Periodontal Implant Sci. 2024;54(2):108–21.
- 6. Pickert FN, Spalthoff S, Gellrich NC, Blaya Tárraga JA. Cone-beam computed tomographic evaluation of dimensional hard tissue changes following alveolar ridge preservation techniques of different bone substitutes: a systematic review and meta-analysis. J Periodontal Implant Sci. 2022;52(1):3–27.
- 7. Kim JH, Susin C, Min JH, Suh HY, Sang EJ, Ku Y, et al. Extraction sockets: erratic healing impeding factors. J Clin Periodontol. 2014;41(1):80–85.
- 8. Kim JH, Koo KT, Capetillo J, Kim JJ, Yoo JM, Ben Amara H, et al. Periodontal and endodontic pathology delays extraction socket healing in a canine model. J Periodontal Implant Sci. 2017;47(3):143–53.
- 9. Kim JJ, Ben Amara H, Chung I, Koo KT. Compromised extraction sockets: a new classification and prevalence involving both soft and hard tissue loss. J Periodontal Implant Sci. 2021;51(2):100–13.
- 10. Kim JJ, Schwarz F, Song HY, Choi Y, Kang KR, Koo KT. Ridge preservation of extraction sockets with chronic pathology using Bio-Oss® Collagen with or without collagen membrane: an experimental study in dogs. Clin Oral Implants Res. 2017;28(7):727–33.
- 11. Kim JJ, Ben Amara H, Park JC, Kim S, Kim TI, Seol YJ, et al. Biomodification of compromised extraction sockets using hyaluronic acid and rhBMP-2: an experimental study in dogs. J Periodontol. 2019;90(4):416–24.
- 12. Lee J, Lee YM, Lim YJ, Kim B. Ridge augmentation using β-tricalcium phosphate and biphasic calcium phosphate sphere with collagen membrane in chronic pathologic extraction sockets with dehiscence defect: a pilot study in beagle dogs. Materials (Basel). 2020;13(6):1452.
- 13. Ben Amara H, Kim JJ, Kim HY, Lee J, Song HY, Koo KT. Is ridge preservation effective in the extraction sockets of periodontally compromised teeth? A randomized controlled trial. J Clin Periodontol. 2021;48(4):464–77.
- 14. Kim JJ, Ben Amara H, Schwarz F, Kim HY, Lee JW, Wikesjö UM, et al. Is ridge preservation/augmentation at periodontally compromised extraction sockets safe? A retrospective study. J Clin Periodontol. 2017;44(10):1051–8.
- 15. Lee J, Yun J, Kim JJ, Koo KT, Seol YJ, Lee YM. Retrospective study of alveolar ridge preservation compared with no alveolar ridge preservation in periodontally compromised extraction sockets. Int J Implant Dent. 2021;7(1):23.
- 16. Koo TH, Song YW, Cha JK, Jung UW, Kim CS, Lee JS. Histologic analysis following grafting of damaged extraction sockets using deproteinized bovine or porcine bone mineral: a randomized clinical trial. Clin Oral Implants Res. 2020;31(1):93–102.
- 17. Lee JS, Cha JK, Kim CS. Alveolar ridge regeneration of damaged extraction sockets using deproteinized porcine versus bovine bone minerals: a randomized clinical trial. Clin Implant Dent Relat Res. 2018;20(5):729–37.
- 18. Nibali L, Sultan D, Arena C, Pelekos G, Lin GH, Tonetti M. Periodontal infrabony defects: Systematic review of healing by defect morphology following regenerative surgery. J Clin Periodontol. 2021;48(1):100–13.
- 19. Chappuis V, Araújo MG, Buser D. Clinical relevance of dimensional bone and soft tissue alterations post-extraction in esthetic sites. Periodontol 2000. 2017;73(1):73–83.
- 20. Schwarz F, Sahm N, Schwarz K, Becker J. Impact of defect configuration on the clinical outcome following surgical regenerative therapy of peri-implantitis. J Clin Periodontol. 2010;37(5):449–55.

Tang et al.,

- 21. Kim YT, Jeong SN, Lee JH. Effectiveness of porcine-derived xenograft with enamel matrix derivative for periodontal regenerative treatment of intrabony defects associated with a fixed dental prosthesis: a 2-year follow-up retrospective study. J Periodontal Implant Sci. 2021;51(4):179–88.
- 22. Lee JS, Choe SH, Cha JK, Seo GY, Kim CS. Radiographic and histologic observations of sequential healing processes following ridge augmentation after tooth extraction in buccal-bone-deficient extraction sockets in beagle dogs. J Clin Periodontol. 2018;45(11):1388–97.
- 23. Bunyaratavej P, Wang HL. Collagen membranes: a review. J Periodontol. 2001;72(2):215-29.
- 24. Percie du Sert N, Ahluwalia A, Alam S, Avey MT, Baker M, Browne WJ, et al. Reporting animal research: Explanation and elaboration for the ARRIVE guidelines 2.0. PLoS Biol. 2020;18(7):e3000411.
- 25. Avila-Ortiz G, Chambrone L, Vignoletti F. Effect of alveolar ridge preservation interventions following tooth extraction: a systematic review and meta-analysis. J Clin Periodontol. 2019;46(Suppl 21):195–223.
- 26. Lim HC, Shin HS, Cho IW, Koo KT, Park JC. Ridge preservation in molar extraction sites with an open-healing approach: a randomized controlled clinical trial. J Clin Periodontol. 2019;46(10):1144–54.
- 27. Zellner JW, Allen HT, Kotsakis GA, Mealey BL. Wound healing after ridge preservation: a randomized controlled trial on short-term (4 months) versus long-term (12 months) histologic outcomes. J Periodontol. 2023;94(4):622–9.
- 28. Couso-Queiruga E, Weber HA, Garaicoa-Pazmino C, Barwacz C, Kalleme M, Galindo-Moreno P, et al. Influence of healing time on the outcomes of alveolar ridge preservation using a collagenated bovine bone xenograft: a randomized clinical trial. J Clin Periodontol. 2023;50(1):132–46.
- 29. Gruber R, Stadlinger B, Terheyden H. Cell-to-cell communication in guided bone regeneration: molecular and cellular mechanisms. Clin Oral Implants Res. 2017;28(9):1139–46.
- 30. Benic GI, Hämmerle CH. Horizontal bone augmentation by means of guided bone regeneration. Periodontol 2000. 2014;66(1):13–40.
- 31. Lee JS, Shin HK, Yun JH, Cho KS. Randomized clinical trial of maxillary sinus grafting using deproteinized porcine and bovine bone mineral. Clin Implant Dent Relat Res. 2017;19(1):140–50.
- 32. Krennmair S, Postl L, Schwarze UY, Malek M, Stimmelmayr M, Krennmair G. Clinical, radiographic, and histological/histomorphometric analysis of maxillary sinus grafting with deproteinized porcine or bovine bone mineral: a randomized clinical trial. Clin Oral Implants Res. 2023;34(8):1230–47.
- 33. Nannmark U, Sennerby L. The bone tissue responses to prehydrated and collagenated cortico-cancellous porcine bone grafts: a study in rabbit maxillary defects. Clin Implant Dent Relat Res. 2008;10(4):264–70.
- 34. Orsini G, Scarano A, Piattelli M, Piccirilli M, Caputi S, Piattelli A. Histologic and ultrastructural analysis of regenerated bone in maxillary sinus augmentation using a porcine bone-derived biomaterial. J Periodontol. 2006;77(12):1984–90.
- 35. Seo GJ, Lim HC, Chang DW, Hong JY, Shin SI, Kim G, et al. Primary flap closure in alveolar ridge preservation for periodontally damaged extraction socket: a randomized clinical trial. Clin Implant Dent Relat Res. 2023;25(2):241–51.